Direct observation of electron self-trapping in $PbCl_2$ crystals

S. V. Nistor,* E. Goovaerts, and D. Schoemaker
Physics Department, University of Antwerp (U.I.A.), B-2610 Antwerpen-Wilrijk, Belgium
(Received 8 April 1993)

Direct experimental evidence is reported for the self-trapping of electrons produced at 80 K by x-ray irradiation or by UV illumination above the band gap in pure, orthorhombic (D_{2h}^{16}) $PbCl_2$ crystals. The ESR analysis demonstrates that the electron is trapped at a pair of nearest-neighbor substitutional Pb^{2+} ions along the a direction, resulting in a paramagnetic Pb_2^{3+} molecular ion with electronic configuration complementary to that of the $(\text{halogen})_2^-$ self-trapped hole center in the alkali halides. The results of this paper suggest that the self-trapped exciton in $PbCl_2$ consists of a hole trapped in an excited orbital around the Pb_2^{3+} center.

I. INTRODUCTION

The possibility of self-trapping of electrons or positive holes in ionic crystals as a result of strong electron-phonon coupling has been considered theoretically already a long time ago.[1,2] Self-trapping of holes has been readily observed and studied extensively by electron-spin-resonance (ESR) in several ionic crystals: The $(\text{halogen}_2)^-$ centers (the V_K centers) in the alkali halides,[3] and Ag^{2+} in[4] AgCl are primary examples. However, no direct observation of electron self-trapping in ionic crystals has been reported so far.

We present here experimental evidence of electron self-trapping in $PbCl_2$ single crystals, at low temperatures. The self-trapping results from localization of the electron in a covalent σ_g-type bond, between two Pb^{2+} ($6s^2$) lattice ions on nearest-neighbor (NN) positions in the a direction of this orthorhombic (D_{2h}^{16}) crystal.[5] The resulting paramagnetic center, hereafter called the self-trapped-electron (STEL) center, can be described as a weakly perturbed Pb_2^{3+} molecular ion, oriented along this crystallographic orientation.

The $PbCl_2$ crystal is ionic in nature, according to results of ionic conductivity measurements,[6] and polarized infra-red (IR) reflectivity and Raman scattering investigations of the lattice dynamics.[7] Electron self-trapping at the cations in the $PbCl_2$ crystal has been suggested earlier in order to explain the the specific properties under illumination in the short-wavelength region (>4.28 eV) at the onset of the fundamental optical absorption:[8] (i) The positive sign of the charge carriers, obtained from photoconductivity studies at 77 K,[9] which suggests that the electrons play the role of the "heavier" charge carriers. (ii) The observation below 200 K of localized excitons at cation sites, as revealed from the large Stokes shift of the luminescence and the spectral structure characteristic for a $6s^2 \rightarrow 6s6p$ excitation of the Pb^{2+} ion in emission and reflectivity measurements.[8,10–12] (iii) The formation of lead colloids by photodecomposition at room temperature (RT), a process that involves as a first step the trapping of electrons at lattice cations resulting in monomer Pb^+ and/or dimer Pb_2^{3+} centers.[13,14]

Various configurations of such paramagnetic centers have been proposed in order to explain the slightly anisotropic ESR spectra, with g factors close to the free-electron value, observed in γ-ray-, x-ray- or ultraviolet (UV)-irradiated lead halides.[14–19] However, all previous interpretations of the ESR spectra are incompatible with the results of recent studies on Pb^+ and Pb_2^{3+} centers in ionic crystals.[20–24] Recently, this was pointed out explicitly.[19]

II. EXPERIMENT

The samples used in the present study were cut from oxygen-free $PbCl_2$ single crystals grown by the Bridgman technique from either proanalysis or ultrapure grade (Pierce-Hicol) $PbCl_2$. No significant difference in these two types of crystals has been observed in our study. Details about crystal growth are given elsewhere.[25] The samples for ESR measurements, of size $3 \times 3 \times 10$ mm^3, were cut from cleaved plates, with their long (rotation) axis parallel to either the a, b, or c crystalline axes, as identified by Laue x-ray diffraction. The irradiations with x-rays (tungsten cathode, 50 kV, 50 mA) and UV light, as well as all other experiments, were performed under ambient red light. The other experimental details are the same as in Ref. 26.

III. RESULTS

A. ESR properties

New anisotropic ESR transitions attributed to the Pb_2^{3+} STEL centers are observed at $T < 60$ K, reaching their maximum concentration after a brief ($\sim$ 10 min) x-ray irradiation at 80 K. No saturation effects of the ESR spectra of the STEL center were observed down to $T = 13$ K, for microwave powers of up to 100 mW. Under the same conditions the ESR spectra from the previously reported A, B, and C centers,[18] with $g \sim 2$, were strongly

saturated. According to thermal pulse annealing experiments the STEL centers are unstable above 130 K and are completely bleached out at $T > 210$ K.

Both the ESR spectra of the Pb_2^{3+} STEL centers for the magnetic field along the a, b, and c crystallographic axes, and the angular variation observed by rotating the magnetic field in the main crystallographic planes, are presented in Figs. 1(i)–1(vi), respectively. The ESR spectrum consists of three multiplets: a central, intense line at $g \sim 1.6$, a doublet with components, which are symmetrically situated with respect to the central line, and a three-line multiplet with very small intensity (as shown below they belong to a quadruplet with a line hidden under the intense central line). Members of a given multiplet possess approximately equal intensities. All components exhibit reduced linewidths $\Delta H_0 = (g/g_0)\Delta H = (5.5 \pm 0.3)$ mT (ΔH is the measured linewidth), virtually independent of temperature in the 12–50 K range. The ratio of the integrated intensities of the three groups of lines is roughly 16:8:1.

B. Analysis of the ESR spectra

The structure of the ESR spectra and the angular variation and splitting of the various ESR lines observed by rotating the magnetic field in the main crystalline planes can be explained by considering the magnetic and structural properties of a Pb_2^{3+} molecular ion localized on a pair of unperturbed NN cation sites along the a axis of the $PbCl_2$ lattice (see Fig. 2).

Viewed along this crystallographic axis the crystal structure consists[5] of layers of distorted, close-packed halogen ions, with lead ions accommodated in the same bc plane. The lattice parameters are $a = 4.525$ Å,

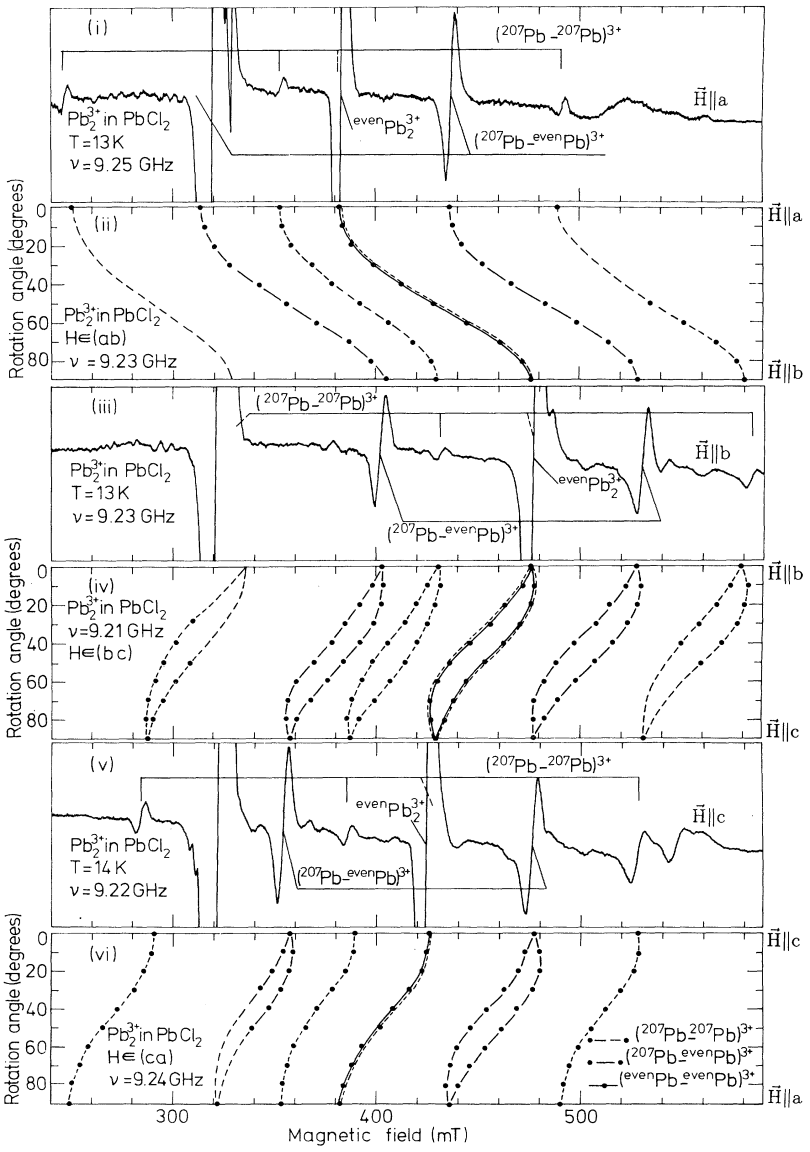

FIG. 1. ESR spectra at T=13 K of the Pb_2^{3+} self-trapped electron (STEL) center in $PbCl_2$ crystals, x-ray irradiated for 10 min at 80 K, for the magnetic field along the crystallographic a (i), b (iii), and c (v) directions. Angular variation of the line positions for the magnetic field rotated in the ab (ii), bc (iv), and ca (vi) planes. The experimental data (dots) are compared to the calculated angular variation (solid line) using the spin-Hamiltonian parameters of Table I.

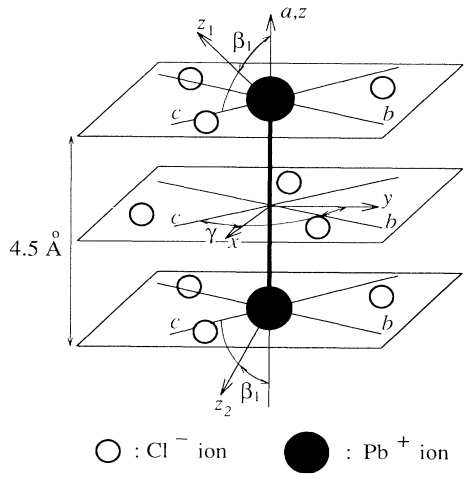

FIG. 2. The schematic model of the Pb_2^{3+} STEL center in $PbCl_2$ and the orientation of the coordinate axes in which the $\underline{g}$ tensor (xyz) and hf $\underline{A}_i$ tensors ($x_iy_iz_i$) are diagonal, as determined from the ESR analysis. Because the hf tensor is axial within experimental accuracy, the orientation of x_i and y_i is experimentally undetermined. Only one of the four possible sign combinations ($\pm\gamma$ and $\pm\beta_1$) of the tilting angles is depicted, i.e., the sense of the bending of the molecular axis is not known.

$b = 7.608$ Å, and $c = 9.030$ Å, and the unit cell contains the $PbCl_2$ molecule twice. The Pb^{2+} sites are monoclinic (C_s) exhibiting only reflection symmetry through the bc plane. There are two types of cation sites in the same layer, which can be transformed into each other by reflection through the ab or ac plane. From the point of view of ESR the two sites are equivalent when the static field is in the ab or ac plane. Any NN pair of Pb^{2+} ions is separated by the lattice distance $a = 4.525$ Å, and the two ions occupy the same type of sites. Each cation is surrounded by three Cl^- ions in the same bc plane, and is sandwiched between two sets of three anions lying above and below in parallel planes, at $\pm a/2$ (Fig. 2).

The ESR spectrum of the Pb_2^{3+} STEL defect is fully described by the spin-Hamiltonian consisting of the Zeeman term and the hyperfine (hf) interactions with two Pb nuclei,

$$\frac{1}{g_0\mu_B}\mathcal{H} = \frac{1}{g_0}\mathbf{H}\cdot\underline{g}\cdot\mathbf{S} + \mathbf{S}\cdot\underline{A}_1\cdot\mathbf{I}_1 + \mathbf{S}\cdot\underline{A}_2\cdot\mathbf{I}_2 \qquad (1)$$

in which $S = 1/2$ and $\underline{A}_1$ and $\underline{A}_2$ are related by reflection symmetry. The second and third term occur only if the corresponding nucleus is the ^{207}Pb isotope (21% natural abundancy), with nuclear spin $I = 1/2$. The other stable isotopes are even (79% natural abundancy) and have zero nuclear spin, $I = 0$. From this the relative concentrations of the possible isotope combinations for the Pb_2^{3+} molecule are readily derived.

The ESR spectrum of the $^{even}Pb_2^{3+}$ species, with relative abundance of 62%, is a singlet line for each of the two types of cation sites, which yield degenerate positions only for specific orientations of the magnetic field. Indeed, for this homonuclear diatomic molecule the bc plane between the two Pb ions is a mirror plane (Fig. 2), and only two inequivalent orientations can occur, corresponding to the two possible types of lattice sites for Pb^{2+}. They are magnetically equivalent when the static field is in the ab or the ca plane, which explains the additional degeneracy observed in Figs. 1(ii) and 1(vi). This spectrum offers the best way to determine the $\underline{g}$-tensor components and the orientation of the principal axes x, y, and z with respect to the crystal axes c, b, and a. One finds that $z \parallel a$, in agreement with the mirror symmetry in our model, and the x and y axes are rotated by $\gamma = \pm 10°$ from the c and b orientations, respectively, as depicted in Fig. 2.

The spectrum of the $(^{even}Pb^{207}Pb)^{3+}$ molecular ion, with a relative abundance of 34%, is described by the first two terms in (1), which results in a doublet structure for each of the central lines. The $\underline{A}$ matrix exhibits the local symmetry of the Pb nucleus, which is lower than that of the molecular ion, and therefore its principal orientations are different from those of the $\underline{g}$ matrix. Because of the inequivalence of the two nuclei, four instead of two inequivalent types of defects occur, which are pairwise related by reflection through each of the crys-

TABLE I. The g values and hf parameters (in mT) of the Pb_2^{3+} self-trapped electron (STEL) center in $PbCl_2$ at 13 K are presented together with the anisotropic and isotropic contributions, ρ_s and A_σ (in mT), to the hf-parameters derived from the molecular analysis, from which also the signs of the hf parameters are derived. The corresponding parameters for two isostructural Pb_2^{3+}-dimer centers in NaCl are listed for comparison.

Center	g_x	g_y	g_z	A_x	A_y	A_z	ρ_s	A_σ
Pb_2^{3+} STEL[a]	1.549	1.379	1.718	−85	−85	+109	+39	−5
in $PbCl_2$	±0.001	±0.001	±0.003	±1	±1	±1		
Pb_2^{3+}(I) [b]	1.438	1.222	1.625	−122	−117	+125	+46	−20
in NaCl	±0.002	±0.002	±0.002	±1	±1	±1		
Pb_2^{3+}(III) [b]	1.469	1.300	1.621	−123	−115	+115	+46	−29
in NaCl	±0.002	±0.002	±0.002	±1	±1	±1		

[a]This work; the principal axes of the $\underline{g}$ tensor, xyz, are rotated with respect to the crystal axes, cba, by the angle $\gamma = \pm 10°$ around the $z \equiv a$ axis, with an estimated accuracy of $\pm 0.5°$. Those of the hf tensor are rotated by the Euler angles $\alpha_1 = 0$, $\beta_1 = \pm 33°$, with an estimated accuracy of $\pm 2°$, while the third Euler angle, γ_1, is experimentally undetermined (see text and Fig. 2).
[b]Reference 22; the ρ_s and A_σ values have been recalculated.

talline planes ab, bc, and ca. As shown in Fig. 1, the expected additional splitting is observed in the ca plane, but not in the ab plane. The hf-tensor components and its principal directions x_1, y_1, and z_1, as well as refined g values, were determined by a computer diagonalization and fitting procedure involving 34 measured line positions of the $^{even}Pb_2^{3+}$ and $(^{even}Pb^{207}Pb)^{3+}$ spectra. The resulting values are listed in Table I. The z_1 principal axis of the hf tensor is tilted away from the a direction by $\beta_1 = \pm 33°$ in the ac plane. Within the experimental accuracy of $\pm 2°$, the angle $\alpha_1 = 0$, i.e., the tilting occurs in the ca plane. This feature seems to be accidental, by which we mean unrelated to the local symmetry, and it accounts for the unexpected degeneracy of the ESR lines observed in the ab angular variation [Fig. 1(ii)]. The hf tensor was found to be axial within experimental uncertainties, leaving the third Euler angle, γ_1, undetermined. The signs of the γ and β_1 angles for a given cation site are structurally significant (see Fig. 2), but cannot be inferred from the ESR data.

The weaker ESR spectra of the $^{207}Pb_2^{3+}$ molecular ion, with a relative abundance of only 4%, are described by the full Hamiltonian (1) with the tensors $\underline{A}_1$ and $\underline{A}_2$ related to each other by reflection through the xy (or ca) plane (Fig. 2). The principal values and orientations of the g and hf tensors, as determined from the singlet and doublet spectra (Table I), were employed to predict the positions of the resulting quadruplet of ESR lines. Three of the transitions could be traced in the experimental spectra [see Figs. 1(i), 1(iii), and 1(v)]. As shown in Figs. 1(ii), 1(iv), and 1(vi), their angular variations did agree accurately with the calculated ones, which confirms our interpretation. The calculation also explains the seemingly absent fourth component, which, within the observed linewidth, coincides with the position of the intense $^{even}Pb_2^{3+}$ transition. As in the $^{even}Pb_2^{3+}$ case, the $^{207}Pb_2^{3+}$ defect possesses mirror symmetry through the bc plane, and the spectra with the static field in the ca or ab plane exhibit the corresponding degeneracy.

C. Optical experiments

Additional evidence favoring the electron-trapping formation mechanism has been obtained from production experiments with UV light at 80 K. In a first type of experiment the $PbCl_2$ sample was illuminated with broadband UV light at $\simeq 5.17$ eV produced by an Osram HBO-200 high-pressure mercury lamp, a focalizing quartz lens and an ARC-240 interference reflection filter, with maximum transmittance of 40% at 240 nm (intensity reduced to 20% at $\pm$ 40 nm). With such a setup, ESR signals attributed to the STEL centers have been obtained after 20 min of continuous irradiation, resulting in maximum concentrations of about 10% compared to the x-ray irradiated samples. The ESR signals could be optically bleached in a few seconds by removing the optical filter and than again restored to the initial intensity by resetting the filter. The difference in the maximum attainable population of the STEL centers obtained by x-ray irradiation and by UV-illumination results from the difference in the penetration depth, which is about ten times smaller for $\simeq 5.17$ eV photons than for the 50 kV x-rays.

In a second experiment the illumination was performed with monochromatic UV light at 4.66 eV ($\lambda = 266$ nm) obtained as the fourth harmonic of a pulsed Nd:YAG laser, supplying an average power of up to 50 mW on the sample. No ESR signals of the STEL centers could be observed even after 1 h of illumination, although the estimated light intensity was two orders of magnitude higher than in the experiments with broadband UV light.

The results of the UV-irradiation experiments strongly support the formation mechanism by electron trapping. Indeed, as shown by photoconductivity[9] and optical studies,[10,11] the illumination with 4.66-eV photons corresponds to optical absorption in the localized excitonic band where no conduction electrons are produced. Illumination around 5.17 eV excites the electrons in the conduction band, from where they are self-trapped at cation sites, resulting in Pb_2^{3+} centers.

Special precautions are to be taken in the optical experiments in order to avoid illumination with light in the visible range. As we found in separate bleaching experiments performed at low temperatures ($T < 60$ K) on x-ray-irradiated samples, the STEL centers are easil bleached out by illumination in the (470–670)-nm range, with maximum effect between 550 and 640 nm. This may be one of the reasons why the Pb_2^{3+} STEL centers were not detected in previous ESR studies.

IV. DISCUSSION

The identification of the STEL center with a Pb_2^{3+} defect is supported by the close correspondence of the g values and the hf parameters with those of the Pb_2^{3+} dimer centers, previously reported[22] in x-ray-irradiated NaCl:Pb^{2+} crystals (see Table I). The lowest molecular orbital of this molecule is complementary to that of the self-trapped hole, or V_K-, center in the alkali halides,[27] which consists of a $(\text{halogen}_2)^-$ molecular ion. The molecular ground orbital is singly occupied and constructed mainly from the $6p$ orbitals of the lead ion, with admixture of s orbitals, $\sigma_g = \alpha_g[6s(1) + 6s(2)] + \beta_g[6p_z(1) - 6p_z(2)]$. It is separated by the energies E_{1g} and E_{2g} from the excited $\pi_{u,x}$ and $\pi_{u,y}$ orbitals, respectively, which are admixed by the spin-orbit interaction. This can be dealt with in a second-order perturbation calculation.

The g and hf parameters of the STEL center were analyzed employing the same procedure as in Ref. 22. In an axial approximation, the hf parameters are expressed in terms of the g shifts, $\Delta g_\perp = g_0 - g_\perp$ and $\Delta g_\parallel = g_0 - g_\parallel$, and of ρ_s and A_σ, the anisotropic and isotropic contributions, respectively, of the hf interaction with the ^{207}Pb nuclei. The resulting ρ_s and A_σ values are given in Table I, and compared with those of the Pb_2^{3+} dimer centers in NaCl. Sign combinations of the hf parameters in the spin-Hamiltonian, other than indicated in this table, lead to unacceptable values of the anisotropic contribution ρ_s. The latter is lower for the Pb_2^{3+} dimer in $PbCl_2$ than in NaCl by about 15%, which suggests a larger delocaliza-

tion of the trapped electron. In both cases, the value is close to half of the atomic ρ_s parameter of the Pb^+ defects in KCl,[20,21] reflecting the spread of the valence electron over the two Pb^{2+} ions in the dimer case. The isotropic hf contribution A_σ is the sum of a positive Fermi contact term, A_σ^s, which results from s mixing in the σ_g ground-state molecular orbital, and a negative part A_σ^e originating from exchange polarization of the inner electrons. The less negative A_σ value determined for Pb_2^{3+} in $PbCl_2$ compared to NaCl, points to a larger s mixing in the σ_g ground-state orbital.

The electron self-trapping on a pair of substitutional cations is further supported by the production properties, which suggest that the mechanism is simple trapping of electrons at the Pb^{2+} cations. Indeed, the production of the Pb_2^{3+} centers at low temperatures, with maximum concentration reached after a very short (10 min) irradiation time, makes it very unlikely that vacancies and interstitials would be involved in the formation and structure of this defect.

Hole self-trapping occurs on pairs of halogen ions in the alkali halides forming a $\langle 110 \rangle$-oriented $(\text{halogen}_2)^-$ molecule ion and on the silver ion in silver chloride forming a planar $(AgCl_4)^{2-}$ molecule ion. In each of these cases, the outer orbitals of the corresponding ions, $3p$ of the Cl^- and $4d$ of the Ag^+, respectively, contribute strongly to the highest valence band of the crystal. Our observation of electron self-trapping on neighboring Pb^{2+} cations in $PbCl_2$ indicates that the crystal conduction band originates predominantly from the $6p$ orbitals of the Pb^{2+}, in agreement with previous reports.[11] Detailed energy-band calculations are needed for a better understanding of electron self-trapping in $PbCl_2$.

In many ionic crystals such as the alkali halides, the self-trapped hole may momentarily trap an electron in an excited orbital resulting in the formation of a self-trapped exciton. Through a non-radiative decay process the excitons are responsible for the production of primary defects such as the F, H, and V_K centers.[28]

The discovery of the self-trapped electron in $PbCl_2$ suggests the possibility of forming excitons by trapping of a hole in an excited orbital. Such excitons may explain the results of luminescence and polarized reflection measurements in lead halides.[10–12,29,30]

Excitons in which the electron plays the role of the heavier component may also be responsible for alternative paths in defect creation by radiolysis in ionic crystals such as lead halides, mercury halides and other layered structures.[31–33]

ACKNOWLEDGMENTS

The authors are grateful to Professor J. Van Landuyt for permission to use the x-ray-diffraction equipment, to Dr. A. Bouwen for expert experimental assistance and C. D. Mateescu for help in growing the single crystals. One of the authors (S.V.N.) is indebted to the Belgian Ministry of Science Policy (DPWB) for financial support. This work was supported by the Belgian science supporting agencies IIKW and NFWO.

* On leave from the Institute of Atomic Physics, Bucuresti, Romania.

[1] L. Landau, Phys. Z. Sowjetunion **3**, 664 (1933).

[2] R. W. Gurney and N. F. Mott, Proc. Phys. Soc. **49** (Suppl.), 32 (1937).

[3] T. G. Castner and W. Känzig, J. Phys. Chem. Solids **3**, 178 (1957).

[4] M. Hohne and H. Stasiw, Phys. Status Solidi **25**, K55 (1968); **28**, 247 (1968).

[5] H. Braekken, Z. Krist. **83**, 222 (1932).

[6] K. J. De Vries and J. H. Van Santen, Physica **29**, 482 (1963).

[7] C. Carabatos-Nedelec, F. Brehat, and B. Wyncke, Infrared Phys. **31**, 611 (1991).

[8] W. C. De Gruijter, J. Solid State Chem. **6**, 151 (1973).

[9] J. F. Verwey and N. G. Westerink, Physica **42**, 293 (1969).

[10] V. G. Plekhanov, Fiz. Tverd. Tela (Leningrad) **13**, 3687 (1971) [Sov. Phys. Solid State **13**, 3112 (1972)]; Phys. Stat. Solidi B **57**, K55 (1973).

[11] G. Liidja and V. L. Plekhanov, J. Luminesc. **6**, 71 (1973), and earlier references cited therein.

[12] M. Fujita, H. Nakagawa, K. Fukui, H. Matsumoto, T. Miyanaga, and H. Watanabe, J. Phys. Soc. Jpn. **60**, 4393 (1991).

[13] J. F. Verwey, J. Phys. Chem. Solids **31**, 163 (1970).

[14] W. C. De Gruijter and J. Kerssen, J. Solid State Chem. **5**, 467 (1972).

[15] A. V. Patankar and E. E. Schneider, J. Phys. Chem. Solids **27**, 575 (1966); Proc. Brit. Ceram. Soc. **9**, 97 (1967).

[16] J. Arends and J. F. Verwey, Phys. Status Solidi **23**, 137 (1966).

[17] W. C. De Gruijter and J. Kerssen, Solid State Commun. **10**, 837 (1972).

[18] J. Kerssen, W. C. De Gruijter, and J. Volger, Physica **70**, 375 (1978).

[19] P. G. Baranov and J. Rosa, Solid State Commun. **74**, 647 (1990).

[20] E. Goovaerts, S. V. Nistor, and D. Schoemaker, Phys. Rev. B **28**, 3712 (1983).

[21] I. Heynderickx, E. Goovaerts, S. V. Nistor, and D. Schoemaker, Phys. Status Solidi B **136**, 69 (1986).

[22] I. Heynderickx, E. Goovaerts, and D. Schoemaker, Phys. Rev. B **36**, 1843 (1987).

[23] M. Fockele, F. Lohse, J. M. Spaeth, and R. H. Bartram, J. Phys: Condens. Matter **1**, 13 (1989).

[24] E. Goovaerts, S. V. Nistor, and D. Schoemaker, J. Phys: Condens. Matter **4**, 9259 (1992).

[25] S. V. Nistor, M. Stefan, and I. Ursu, Solid State Commun. **85**, 983 (1993).

[26] E. Goovaerts, J. Andriessen, S. V. Nistor, and D. Schoemaker, Phys. Rev. B **24**, 29 (1981).

[27] D. Schoemaker, Phys. Rev. B **7**, 786 (1973).

[28] B. Henderson and F. G. Imbush, *Optical Spectroscopy of Inorganic Solids* (Clarendon, Oxford, 1989).

[29] K. Polak, D. J. S. Birch, and M. Nikl, Phys. Status Solidi **145**, 741 (1988).
[30] M. Nikl, D. J. S. Birch, and K. Polak, Phys. Status Solidi B **165**, 611 (1991).
[31] M. R. Tubbs, Phys. Status Solidi B **49**, 11 (1972); **67**, 11 (1975).
[32] Z. Bryknar, M. Procio, and C. Barta, Czech. J. Phys. B **37**, 1301 (1987).
[33] Z. Bryknar, Cryst. Latt. Def. Amorph. Mater. **17**, 219 (1987).